Jpn. J. Infect. Dis., 70, 383–387, 2017

Original Article

Dengue Virus-Induced Reactive Oxygen Species Production in Rat Microglial Cells

Lattapon Suwanprinya[1], Noppawan Phumala Morales[1], Pimtip Sanvarinda[1], Hamady Dieng[4], Tamaki Okabayashi[2,5]**, and Ronald Enrique Morales Vargas[3]*

[1]*Department of Pharmacology, Faculty of Science;* [2]*Mahidol-Osaka Center for Infectious Diseases (MOCID);* [3]*Department of Medical Entomology, Faculty of Tropical Medicine, Mahidol University, Bangkok, Thailand;* [4]*Institute of Biodiversity and Environmental Conservation, Universiti Malaysia Sarawak, Sarawak, Malaysia; and* [5]*Department of Virology, Research Institute for Microbial Diseases, Osaka University, Osaka, Japan*

SUMMARY: Encephalitis has been described worldwide as a severe complication in patients infected by dengue virus. Reactive oxygen species (ROS) production is a key mechanism involved in the neuronal damage caused by viral encephalitis. In the present study, the capability of dengue virus serotypes 2 (DENV2) and DENV4 to induce ROS production was investigated in a rat microglial cell line, HAPI cells. The cells were infected with DENV2 and DENV4 at a multiplicity of infection of 0.1 for a 2-h adsorption period. Japanese encephalitis virus (JEV) was used as the reference. DENV2- and DENV4-induced microglial activation and significantly increased ROS production corresponded to decreased cell viability. The activity of DENV4 was significantly higher than the activities of DENV2 and JEV at 48 and 72 h post infection. DENV4 partly induced ROS production via an iron-induced Fenton reaction, as demonstrated by the treatment with an iron chelator, deferiprone. Despite the induction of increased inducible nitric oxide synthase expression and nitric oxide (NO) production by JEV, DENV2, and DENV4 did not induce NO production, suggesting the activation of different pathways in response to infections by different viruses. In conclusion, DENV2 and DENV4 have the capability to induce ROS production and activate microglia, which have been reported as the key components of neuronal damage.

INTRODUCTION

Dengue virus (DENV) is an arthropod-borne virus of the *Flaviviridae* family. Four serotypes of DENV (DENV1–4) cause a broad range of disease severity such as dengue fever, dengue hemorrhagic fever, and dengue shock syndrome. DENV2 commonly circulates in several regions of the world, especially in Thailand and Southeast Asia, and it is related to outbreaks of a severe form of dengue. Although DENV4 is generally found at low frequency, DENV4 and DENV2 have been reported in relation to severity of secondary infections (1,2). Increasing evidence of encephalitis in patients with dengue infection has been reported worldwide. In 2009, the World Health Organization (WHO) released new dengue guidelines that consider central nervous system (CNS) complications in clinical cases as severe dengue (3,4). In addition, experiments in mouse models demonstrated the capability of DENV2 and DENV4 isolates to induce encephalitis (5,6). Therefore, dengue encephalitis should be of concern in dengue endemic area.

Japanese encephalitis virus (JEV) infection is a major cause of viral encephalitis among children in Southeast Asia (7). The molecular mechanisms of JEV-induced neuronal damage have been elucidated. One of the key mechanisms of neuronal damage is reactive oxygen species (ROS) production in CNS. ROS such as hydroxyl radicals and superoxide are critical in the apoptosis and necrosis of infected cells. Their production has been demonstrated in neutrophils (8), neuroblastoma (9), and astrocytes (10).

The major sources of ROS in CNS are microglial cells, which are the resident macrophages responsible for homeostasis regulation and defense against injury. Microglial cells are usually beneficial and support neuronal survival through the secretion of growth factors and anti-inflammatory cytokines. Activated microglial cells produce various pro-inflammatory mediators, nitric oxide, and ROS; however, their prolonged activation can be a hallmark of many neurodegenerative disorders (11). In case of JEV, microglia are considered to be the most important players that may act as a Trojan horse for virus infiltration into CNS and release several factors and cytokines that ultimately result in neuronal death (12,13).

Because microglial activation and ROS production are important mechanisms in viral encephalitis, we studied the response of a rat microglial cell line, highly aggressive proliferating immortalized (HAPI) cells, to DENV infection. HAPI cells exhibit several microglial characteristics and are comparable to rat primary microglia in experiments assessing phagocytosis and nitric oxide

Received May 20, 2016. Accepted November 4, 2016. J-STAGE Advance Publication December 22, 2016. DOI: 10.7883/yoken.JJID.2016.236

*Corresponding author: Mailing address: Department of Medical Entomology, Faculty of Tropical Medicine, Mahidol University, Bangkok 10400, Thailand. Tel: +66-2-3069177, Fax: +66-2-6435582, E-mail: ronald.mor@mahidol.ac.th

**Present address: Laboratory of Veterinary Microbiology, Department of Veterinary Science, Faculty of Agriculture, Miyazaki University, Miyazaki, Japan.

(NO) and ROS production (14,15). The responses of HAPI cells to DENV2 and DENV4 infection were analyzed because of the far differences in genetic and phenotypic characteristics of 2 serotypes (16,17). DENV2 and DENV4 capacity to induce HAPI cells may be used to study DENV-induced encephalitis.

MATERIALS AND METHODS

Viruses: JEV (Nakayama strain), DENV2 (16681 strain), and DENV4 (H241 strain) were used for infection experiments throughout this study.

Cell culture and virus infection: HAPI cells were generously provided by Prof. James R. Conor (Department of Neuroscience and Anatomy, Hershey Medical Center, Hershey, PA, USA). HAPI cells were plated at a seeding density of 1×10^4 and 2×10^5 cells/well in 96- and 6-well plates, respectively. Cells were maintained in phenol red-free Dulbecco's modified Eagle's medium (DMEM; Gibco-BRL, Grand Island, NY, USA) supplemented with 2.5% fetal bovine serum (FBS; PAA Laboratories, Queensland, Australia) at 37°C in a humidified incubator under 5% CO_2 and 95% air for 24 h before being infected with JEV, DENV2, or DENV4 at a multiplicity of infection (MOI) of 0.1 for 2 h at 37°C. Following adsorption, unbound virus was removed, and cells were washed with phosphate-buffered saline (PBS), replaced with fresh medium, and further incubated at 37°C.

We used 1 μg/ml lipopolysaccharide (LPS, *Escherichia coli* serotype 026:B6; Sigma-Aldrich, St. Louis, MO, USA) as a positive control. To evaluate the involvement of iron-induced ROS production (Fenton reaction), 1 μM deferiprone (Government Pharmaceutical Organization [GPO], Bangkok, Thailand), a membrane permeable iron chelator, was co-incubated with the virus and supplied to the medium throughout the study period. Cell viability, intracellular ROS production, and other parameters were determined at 24, 48, and 72 h post infection (hpi).

Intracellular ROS production: Intracellular ROS production was measured using 2′,7′-dichlorodihydrofluorescein diacetate (H_2DCFH-DA; Molecular Probe, Eugene, OR, USA) as a fluorescent probe (18). Following the removal of the medium at the indicated post-infection times, 20 μM H_2DCFH-DA was added in DMEM and incubated at 37°C for 30 min in the dark. Cells were then washed with 1 × PBS and fresh DMEM was added. Fluorescence intensity was immediately analyzed at an excitation wavelength of 485 nm and an emission wavelength of 528 nm using the Synergy HT Multi-Detection Microplate Reader (Bio-Tek, Winooski, VT, USA). Intracellular ROS production was normalized to cell viability and expressed as a fold change with respect to the control.

Cell viability: Cell viability was determined by the quantitative colorimetric 3-(4,5-dimethylthiazol-2-yl)-2,5-diphenyltetrazolium bromide (MTT) assay (19). After ROS determination, the medium was removed, and cells were incubated with 1 mg/ml MTT at 37°C for 3 h. The formation of formazan crystals was measured at an absorbance of 562 nm and 630 nm using the Synergy HT reader. Cell viability was expressed as a percentage with respect to the control.

NO production: NO production was determined by measuring the released nitrates and nitrites in the culture medium using 2,3-diaminonaphthalene (2,3-DAN; Molecular Probe) as a fluorescence probe (20). In brief, 150 μl medium was added to 2,3-DAN in HCl and incubated at 30°C for 5 min in the dark. After the addition of 3.0 N NaOH, the mixture was immediately measured at an excitation wavelength of 365 nm and an emission wavelength of 410 nm with the Synergy HT reader. The concentration of NO was calculated using a sodium nitrite standard curve.

Expression of inducible nitric oxide synthase (iNOS): Expression of iNOS was determined using western blot analysis. Protein samples were collected following cell lysis with RIPA buffer (50 mM Tris-HCl [pH 7.4], 150 mM NaCl, 1% Triton X-100, 0.1% sodium deoxycholate, 5 mM EDTA, 30 mM Na_2HPO_4, 50 mM NaF mixed with 1% protease inhibitor cocktail [Cell Signaling, Danvers, MA, USA], and 0.5% $NaVO_4$). The protein concentration was determined by the Lowry method using bovine serum albumin as the standard.

We used 40 μg of protein sample, electrophoresed them on a 10% sodium dodecyl sulfate (SDS)-polyacrylamide gel using 1 × running buffer (1.5 M Tris-HCl, pH 8.8) and transferred to a 0.2-μm polyvinylidene difluoride membrane (Immobilon-PSQ; Millipore, Bedford, MA, USA). The membrane was blocked with 5% skimmed milk (Hardy Diagnostics, Santa Maria, CA, USA) in 1 × PBS with Tween 20 (PBST) for 1 h and hybridized with a rabbit antibody for iNOS ((Santa Cruz Biotechnology, Santa Cruz, CA, USA; 1:1000) or a mouse antibody for β-actin (Cell Signaling; 1:1000) at 4°C overnight. After thoroughly washing with 1 × PBST, the membrane was incubated with anti-rabbit or anti-mouse IgG conjugated to horseradish peroxidase (Cell Signaling; 1:5000) for 1 h at room temperature. The membrane was visualized using Clarity Western ECL substrate (Bio-Rad, Hercules, CA, USA) and exposed to MX-B green X-ray film (Kodak, Rochester, NY, USA). The immunoblot signals were quantified by measuring the intensity of each band using the ImageJ software (Bethesda, MD, USA). β-Actin was used as an internal control, and the results were represented as a fold change with respect to the control.

Statistical analysis: The statistical analysis was performed using the SPSS software ver. 19.0. (Chicago, IL, USA) The data were expressed as the mean ± standard error of mean (SEM) of at least 4 replicates in 2 independent experiments. The comparisons were analyzed by one-way ANOVA and Tukey's honestly significant difference (HSD) test as a post-hoc test or the Mann-Whitney *U* test. Spearman's test was used for correlation analysis. The differences were considered significant when $p < 0.05$.

RESULTS

Evidence of microglial activation was demonstrated by morphological changes. In the resting stage, HAPI cells are spherical in shape, with small processes and transform to an amoeboid phagocytic shape in response to stimuli such as LPS. Following infections with JEV, DENV2, and DENV4, the shape of HAPI cells changed from spherical to amoeboid with long processes (Fig. 1). These morphological changes were observed as early as

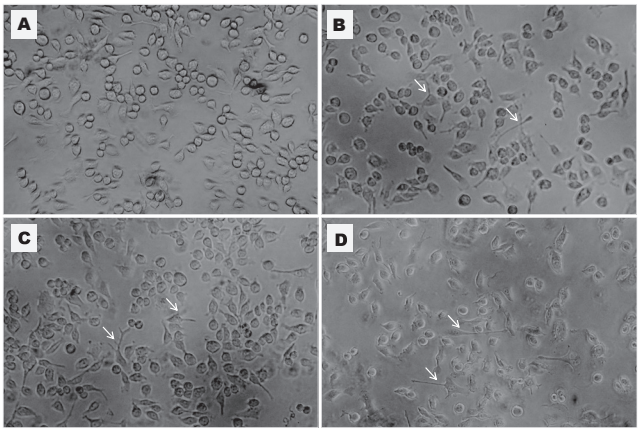

Fig. 1. Microscopic observation of HAPI cells (A) and following infection with JEV (B), DENV2 (C), and DENV4 (D) at 6 hpi. HAPI cells were cultured in DMEM supplemented with 2.5% FBS at a density of 1×10^4 cells/well on 96-well plates for 24 h prior to infection at an MOI of 0.1 for a 2-h absorption period. The original images were taken at 20 × magnification. Arrows indicate activated HAPI cells.

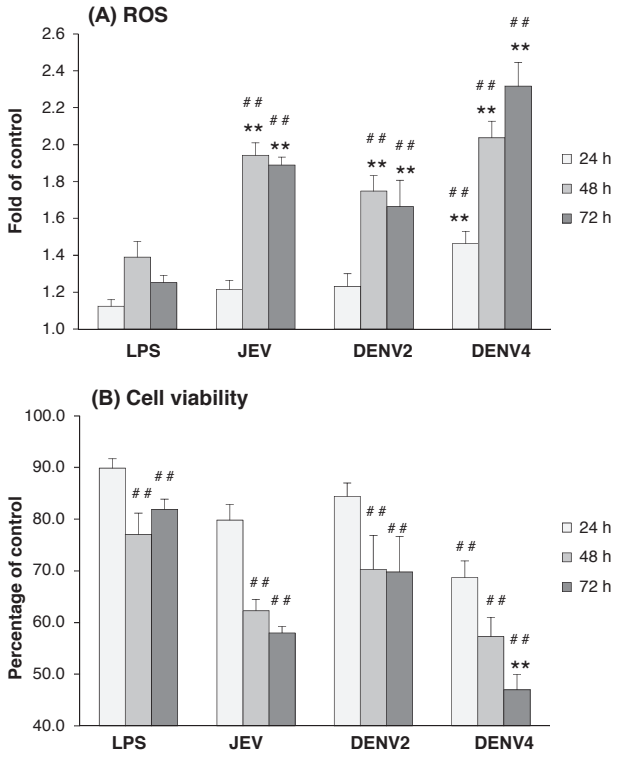

Fig. 2. Effects of JEV, DENV2, and DENV4 on ROS production (A) and cell viability (B). HAPI cells were infected with viruses at an MOI of 0.1 for a 2-h adsorption period. LPS (1 μg/ml) was used as a positive control. ROS and cell viability were determined at 24, 48, and 72 hpi. Data are expressed as the mean ± SEM ($n = 8$). The comparisons were analyzed by one-way ANOVA and Tukey's HSD test as a post-hoc test; $^{\#\#}p < 0.001$ compared with control and $^{**}p < 0.001$ compared with LPS at the respective time.

6 hpi.

JEV, DENV2, and DENV4 enhanced intracellular ROS production and resulted in decreased cell viability (Fig. 2). As a positive control, LPS induced ROS production of approximately 1.2–1.4 fold with respect to the negative control. The reference virus JEV potently activated ROS production, which significantly increased to 2 fold at 48 and 72 hpi ($p < 0.001$ when comparing with a negative control and LPS). Compared with the negative control and LPS, DENV2 significantly induced ROS production at 48 and 72 hpi ($p < 0.001$). Although DENV2 showed less activity than JEV, there was no statistically significant difference between JEV and DENV2.

In contrast, a progressive increase in ROS production was observed following infection with DENV4. ROS production was approximately 1.5-fold greater at 24 hpi ($p < 0.001$ when comparing with a negative control and LPS) and significantly increased to 2.0 and 2.4 fold at 48 and 72 hpi, respectively ($p < 0.001$). In addition, DENV4 showed a significantly higher activity compared with JEV ($p < 0.05$ at 72 hpi) and DENV2 ($p < 0.001$ at 48 and 72 hpi).

In accordance with the increased ROS production, cell viability gradually decreased following infection with viruses. The decrease in cell viability was pronounced with DENV4. Correlation analysis demonstrated a relationship between cell viability and intracellular ROS production (JEV, $r = -0.801$, $p < 0.001$; DENV2, $r = -0.604$, $p < 0.001$; DENV4, $r = -0.746$, $p < 0.001$).

ROS includes several species of free radical and

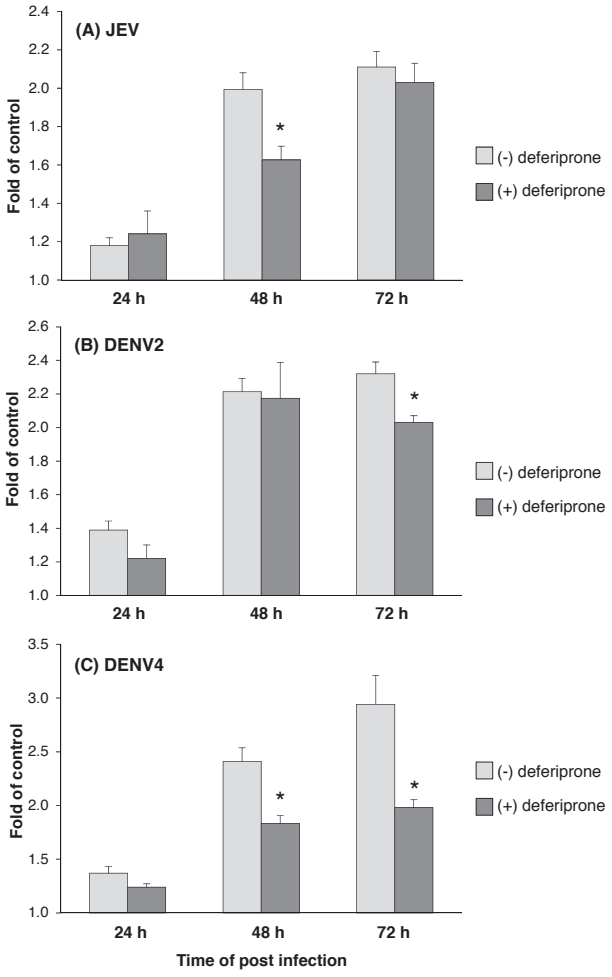

Fig. 3. Effect of an iron chelator, deferiprone, on ROS production in HAPI cells infected with JEV (A), DENV2 (B), and DENV4 (C). HAPI cells were infected with virus at an MOI of 0.1 for a 2-h adsorption period. Following removal of the virus, 1 μM deferiprone was added to the culture medium and incubated throughout the experiment. Data are expressed as the mean ± SEM ($n = 8$). The comparisons were analyzed by the Mann–Whitney U test; $^{*}p < 0.05$.

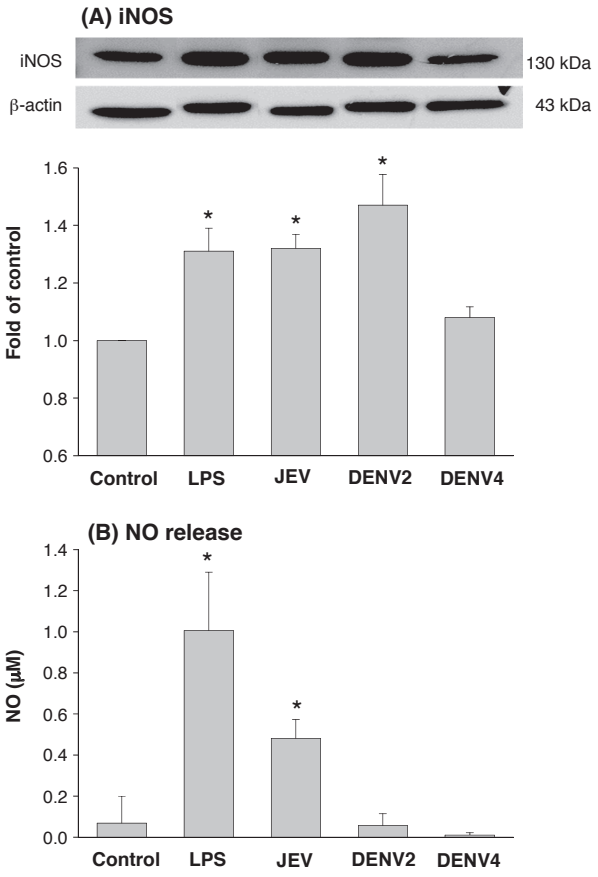

Fig. 4. Expression of the iNOS protein (A) and release of NO (B) following the infection of HAPI cells with JEV, DENV2, and DENV4. HAPI cells were infected with viruses at an MOI of 0.1 for a 2-h adsorption period. Expression of iNOS and the level of NO in the medium were determined at 24 hpi. Data are expressed as the mean ± SEM ($n = 3$). The comparisons were analyzed by the Mann–Whitney U test; * $p < 0.05$.

non-radical molecules. In this study, the involvement of the iron-induced Fenton reaction was evaluated. Supplementing an iron chelator, deferiprone, suppressed the oxidative response induced by all the viruses examined (Fig. 3). However, the susceptibility to deferiprone was higher in cells infected with DENV4 (Fig. 3C). ROS decreased by 30% and 10% in cells infected with DENV4 and DENV2, respectively. In addition, treatment with deferiprone significantly increased (approximately 10%) the viability of cells infected with DENV4 at 48 and 72 hpi ($p < 0.05$; data not shown).

The protein expression of iNOS and release of NO were determined, and the results are shown in Fig. 4. As a positive control, LPS and JEV enhanced iNOS expression by 1.2–1.4 fold compared with the control. DENV2 significantly increased the expression of iNOS, whereas DENV4 infection did not show any detectable effect. In accordance with iNOS, NO release significantly increased with LPS and JEV but not with DENV4. In case of DENV2, NO production was low, despite a significantly increased expression of iNOS.

DISCUSSION

ROS production has been demonstrated in several viral infections, including those caused by human immunodeficiency virus, influenza virus, and JEV (21). The present study, using the H_2DCFH-DA fluorescent probe, demonstrates the capability of DENV2 and DENV4 to induce ROS production when the rat microglial cells were infected. The extent of intracellular ROS production during DENV infection was similar to that during JEV infection; The H2DCFH-DA fluorescent probe is widely used to evaluate intracellular ROS level and is useful as a marker for cellular oxidative stress. It is oxidized by hydrogen peroxide (H_2O_2), hydroxyl radical ($HO^{\bullet}$), peroxyl radical ($ROO^{\bullet}$), and peroxynitrite ($ONOO^{-}$) but not by superoxide ($O2^{\bullet -}$) and NO (22).

The species and mechanism of ROS production during viral infection have not yet been clearly elucidated. An experiment on JEV infection has demonstrated the generation of $O2^{\bullet -}$ in rat cortical glial cells (23). The binding of cytokines, pathogens, or toxins to their receptors triggers rapid intracellular production of ROS, especially $O2^{\bullet -}$ and H_2O_2, which play important roles in redox-dependent signaling pathway of chemokine and cytokine production as well as in apoptosis (24). Furthermore, some viruses interfere with intracellular iron metabolism; this may trigger the Fenton reaction, producing $HO^{\bullet}$, highly toxic to cells (25,26). Therefore, depending on the type of virus, host cell, and ROS, the increase in ROS production may result in a wide range of cellular responses. ROS may have beneficial effects such as promoting the host defense system; however, it may facilitate viral replication, and excessive ROS production causes oxidative stress, cell damage, and ultimately cell death (27).

In our study, all viruses activated microglia and induced ROS production. According to the mechanisms of ROS production described above, there may be two phases of ROS production. In the first phase, for example during viral attachment and entry, components of virus particle *per se* may induce rapid ROS production and trigger signaling pathways of pro-inflammation cytokine production and iNOS expression (24,25). The second phase (48 and 72 hpi) could be a consequence of the release of oxidative products such as cytokines, NO, and other components from damaged cells involved in iron metabolism and mitochondrial functions of the host cells (28, reviewed in 21). Although increased ROS production resulted in oxidative stress and cell death, the oxidative susceptibility and cell responses were different upon exposure to the different viruses.

DENV4 was highly toxic to microglial cells; however, among all the viruses, DENV4 had no effect on iNOS expression. This result may be explained by the high level of intracellular ROS sufficient to cause cell damage and death during early infection. In addition, Li and Engelhardt (29) have reported that a high concentration of H_2O_2 inhibited nuclear factor kappa B (NF-κB) activity. Thus, we may speculate that a high level of ROS production may inversely inhibit iNOS expression.

On the other hand, infection with JEV and DENV2 resulted in enhanced iNOS protein expression. ROS has been implicated in the activation of NF-κB, which plays a central role in the expression of iNOS (30). Enhanced iNOS expression in relation to ROS and NF-κB has been demonstrated in several JEV-infected cell lines, including neuroblastoma and microglia (13) as well as in mouse models (31,32). Although DENV2 revealed an increase in iNOS expression, the pathway of iNOS

induction may not be the same during DENV and JEV infections. In some viral diseases, iNOS expression is regulated by interferon (IFN)-γ and in other cases, viral components directly induce iNOS. Furthermore, the level of NO production is important in determining its biological effect. Physiological levels (nM) function as signal transduction molecules, whereas higher levels act as toxic molecules (25).

The toxicity of NO results from the reaction of NO with $O2^{\bullet-}$, yielding $ONOO^{-}$. Depending on the concentration (and disease situation), NO acts as an anti-inflammatory or pro-inflammatory factor. Because NO inhibits RNA virus replication, NO is known as an antiviral molecule; thus, high iNOS levels with NO production could be a target for the treatment of JEV (33).

We also observed that treatment with a membrane permeable iron chelator was effective in reducing ROS production and increasing cell viability during DENV infection, suggesting the involvement of iron in oxidative damage following infection with DENV. It is known that microglial cells express several iron transporters and contain high iron content. The misregulation of iron in microglia is involved in several neurodegenerative disorders. Pro-inflammatory cytokines such as tumor necrosis factor α and interleukin 1β, which are released during viral infection, have been demonstrated to be involved in regulation of intracellular iron in astrocytes and microglia (28). Therefore, it will be interesting to explore the role of DENV in iron metabolism in microglia. An iron chelator could be a candidate drug for dengue encephalitis treatment.

In conclusion, we have demonstrated that DENV2 and DENV4 have the capacity to induce ROS production in microglia similarly to JEV. The results pertaining to iNOS, NO release, and the response to the iron chelator suggested the activation of different pathways in response to different viral infections. Thus, our findings may be important for the treatment and management of infectious viral diseases.

Acknowledgments This project was supported by the Office of the Higher Education Commission and Mahidol University under the National Research Universities Initiative. Authors also appreciate the National Research Council of Thailand for partly supporting this project to LS.

Conflict of interest This project was supported by the program of the Japan Initiative for Global Research Network on Infectious Diseases, directed by the Ministry of Education, Culture, Sports, Science and Technology of Japan and by Alfresa Pharma Corporation.

REFERENCES

1. Nisalak A, Endy TP, Nimmannitaya S, et al. Serotype-specific dengue virus circulation and dengue diseases in Bangkok, Thailand from 1973 to 1999. Am J Trop Med Hyg. 2003;68:191-202.
2. Limkittikul K, Brett J, L'Azou M. Epidemiological trends of dengue diseases in Thailand (2000–2011): a systemic literature review. PLoS Negl Trop Dis. 2014;8:e3241.
3. Carod-Artal FJ, Wichmann O, Farrar J, et al. Neurological complications of dengue virus infection. Lancet Neurol. 2013;12:906-19.
4. Soares CN, Cabral-Castro MJ, Peralta JM, et al. Review of the etiologies of viral meningitis and encephalitis in a dengue endemic region. J Neurol Sci. 2011;303:75-9.
5. Amorim JH, Bizerra RSP, Alves RPS, et al. A genetic and pathologic study of DENV2 clinical isolate capable of inducing encephalitis and hematological disturbances in immunocompetent mice. PLoS One. 2012;7:e44984.
6. Velandia-Romero ML, Acosta-Losada O, Castellanos JE. In vivo infection by a neuroinvasive neurovirulent dengue virus. J Neurovirol. 2012;18:374-87.
7. Misra UK, Kalita J. Overview: Japanese encephalitis. Prog Neurobiol. 2010;91:108-20.
8. Srivastava S, Khanna N, Saxena SK, et al. Degradation of Japanese encephalitis virus by neutrophils. Int J Exp Pathol. 1999;80:17-24.
9. Raung SL, Kuo MD, Wang YM, et al. Role of reactive oxygen intermediates in Japanese encephalitis virus infection in murine neuroblastoma cells. Neurosci Lett. 2001;315:9-12.
10. Tung WH, Tsai HW, Lee IT, et al. Japanese encephalitis virus induces matrix metalloproteinase-9 in rat brain astrocytes via NF-κB signalling dependent on MAPKs and reactive oxygen species. Br J Pharmacol. 2010;161:1566-83.
11. Dheen ST, Kaur C, Ling EA. Microglial activation and its implications in the brain diseases. Curr Med Chem. 2007;14:1189-97.
12. Thongtan T, Thepparit C, Smith DR. The involvement of microglial cells in Japanese encephalitis infections. Clin Dev Immunol. 2012;2012:890586.
13. Ghoshal A, Das S, Ghosh S, et al. Proinflammatory mediators released by activated microglia induces neuronal death in Japanese encephalitis. Glia. 2007;55:483-96.
14. Cheepsunthorn P, Radov L, Menzies S, et al. Characterization of novel brain-derived microglial cell line isolated from neonatal rat brain. Glia. 2001;35:53-62.
15. Horvath RJ, Nutile-McMenemy N, Alkaitis MS, et al. Differential migration, LPS-induced cytokine, chemokine and NO expression in immortalized BV-2 and HAPI cell lines and primary microglial cultures. J Neurochem. 2008;107:557-69.
16. Blok J. Genetic relationships of the dengue virus serotypes. J Gen Virol. 1985;66:1323-5.
17. Hannemann H, Sung PY, Chiu HC, et al. Serotype specific differences in dengue virus non-structural protein 5 nuclear localization. J Biol Chem. 2013;288:22621-35.
18. Rastogi RP, Singh SP, Hader DP, et al. Detection of reactive oxygen species (ROS) by the oxidant-sensing probe 2',7'-dichlorodihydrofluorescein diacetate in the cyanobacterium *Anabaena variabilis* PCC 7937. Biochem Biophys Res Commun. 2010;397:603-7.
19. Mosmann T. Rapid colorimetric assay for cellular growth and survival: application to proliferation and cytotoxicity assays. J Immunol Methods. 1983;65:55-63.
20. Nussler AK, Glanemann M, Schirmeier A, et al. Fluorometric measurement of nitrite/nitrate by 2,3-diaminonaphthalene. Nat Protoc. 2006;1:2223-6.
21. Schwarz KB. Oxidative stress during viral infection: a review. Free Radic Biol Med. 1996;21:641-9.
22. Gomes A, Fernandes E, Lima JLFC. Fluorescence probes used for detection of reactive oxygen species. J Biochem Biophys Methods. 2005;65:45-80.
23. Liao SL, Raung SL, Chen CJ. Japanese encephalitis virus stimulates superoxide dismutase activity in rat glial cultures. Neurosci Lett. 2002;324:133-6.
24. Finkel T. Oxidant signals and oxidative stress. Curr Opin Cell Biol. 2003;15:247-54.
25. Akaike T. Role of free radicals in viral pathogenesis and mutation. Rev Med Virol. 2001;11:87-101.
26. Drakesmith H, Prentice A. Viral infection and iron metabolism. Nat Rev Microbiol. 2008;6:541-52.
27. Sauer H, Wartenberg M, Hescheler J. Reactive oxygen species as intracellular messengers during cell growth and differentiation. Cell Physiol Biochem. 2001;11:173-86.
28. Rathore KI, Redensek A, David S. Iron homeostasis in astrocytes and microglia is differentially regulated by TNF-α and TGF-β1. Glia. 2012;60:738-50.
29. Li Q, Engelhardt JF. Interlukin-1β induction of NFκB is partially regulated by H_2O_2-mediated activation of NF-κB-inducing kinase. J Biol Chem. 2006;281:1495-505.
30. Pautz A, Art J, Hahn S, et al. Regulation of expression of inducible nitric oxide synthase. Nitric Oxide. 2010;23:75-93.
31. Mishra MK, Dutta K, Saheb SK, et al. Understanding the molecular mechanism of blood-brain barrier damage in an experimental model of Japanese encephalitis: correlation with minocycline administration as a therapeutic agents. Neurochem Int. 2009;55:717-23.
32. Saxena V, Mathur A, Krishnani N, et al. Kinetics of cytokine profile during intraperitoneal inoculation of Japanese encephalitis virus in BALB/c mice model. Microbes Infect. 2008;10:1210-7.
33. Saxena SK, Mathur A, Srivastava RC. Inducible of nitric oxide synthase during Japanese encephalitis virus infection: evidence of protective role. Arch Biochem Biophys. 2001;391:1-7.